Materials Today Communications 25 (2020) 101479

Contents lists available at ScienceDirect

Materials Today Communications

journal homepage: www.elsevier.com/locate/mtcomm

A dynamic hysteresis model based on Landau phenomenological theory of fatigue phenomenon in ferroelectrics

Xuan He[a,d], Haoyuan Du[a], Zheng Tong[b], Dan Wang[c], Linxiang Wang[a,*], Roderick Melnik[d,e]

[a] State Key Laboratory of Fluid Power and Mechatronic Systems, Zhejiang University, 310027, Hangzhou, China
[b] Research Institute of Petroleum Exploration and Development (RIPED), PetroChina, P. O. Box910, No. 20 Xueyuan Road, 100083, Beijing, China
[c] College of Mechanical and Electrical Engineering, Nanjing University of Aeronautics & Astronautics, 210016, Nanjing, China
[d] MS2Discovery Interdisciplinary Research Institute, Wilfrid Laurier University, Waterloo, ON, N2L 3L5, Canada
[e] BCAM-Basque Center for Applied Mathematics, Alameda De Mazarredo 14, E-48009, Bilbao, Spain

ARTICLE INFO

Keywords:
Ferroelectrics
Hysteretic dynamics
Fatigue
Landau theory

ABSTRACT

In the current paper, the coupled fatigue hysteretic behaviors in ferroelectric ceramics are modeled by a blending a phenomenological hysteresis model with point defects. The time-dependent phenomenological model is employed to capture the hysteresis loops associated with phase transitions. The fatigue hysteresis is modeled by combining the single-crystal model with time functions. The mechanism of fatigue in ferroelectric ceramics is interpreted as an accumulation of residual polarization in the proposed model. Numerical results of static and dynamic hysteretic behaviors are presented and compared to their experimental counterparts. The capability of the proposed model for capturing the fatigue phenomenon is validated.

1. Introduction

Ferroelectric ceramic materials, such as PZT, PLZT, and PMN, are popular in applications areas such as random access memory devices, sensors and actuators, and vibration dampers. They are capable of converting energy reversibly between the electrical and mechanical types by the material itself due to its inherent electro-mechanical coupling properties [1]. In most practical applications, it is generally desirable to have the ferroelectric devices and systems to have as larger strain and electric displacement responses as possible. Therefore, this technical requirement often makes the ferroelectric devices operate under high voltage stimulations (or strong electric fields). Unfortunately, hysteresis loops will occur in the field-polarization (E-P) and field-strain (E-ϵ) relations simultaneously, due to the polarization switching and reorientation caused by the external electric field and mechanical loadings when it is larger than the coercive field [2].

In most cases, ferroelectric devices are facing the problem of performance degradation during their lifetime. Aging [3–5] as well as fatigue [6–8] are the major causes that to be responsible for their performance degradation. The aging phenomenon accounts for the degradation of ceramics properties without external loadings as time goes by, whereas the fatigue phenomenon describes the performance degradation under the high electrical loading and large loading cycle numbers. In the current paper, only the fatigue phenomenon will be investigated and the aging phenomenon is out of the scope of the current studies.

The mechanism of fatigue phenomenon is still open and there is no commonly accepted theory to explain it. Among the existing investigations, some theories at micro-scale have been proposed to explain fatigue at macro-scale and become inspiring. A popular approach to relate a theory is to a temperature function [9], and to attribute the fatigue phenomenon to the pinning of domain walls at structural defects in the material. Some other theories are proposed by attributing the fatigue phenomenon in ferroelectric ceramics to micro-cracking [10], and these kinds of fatigue are irreversible [3]. The common point of these mechanisms is that the internal bias field caused by lattice defects reduces the remnant switchable polarization under the external electrical field.

Different from the micromechanical models, phenomenological models have also been proposed to simulate the fatigue phenomenon at macro-scale. Traditional phenomenological models, such as the Preisach model, have the advantage of being simple in physics and mathematics. However, the hysteresis loops in the electric and mechanical fields for ferroelectric ceramics both have obvious time-dependence, such as creeping or fatigue. It is a tough task to develop a suitable model to capture and quantify all the coupled hysteretic dynamics based on the Preisach model. To overcome the limitation of the Preisach model, a dynamic differential model has been developed by

* Corresponding author.
E-mail address: wanglx236@zju.edu.cn (L. Wang).

https://doi.org/10.1016/j.mtcomm.2020.101479
Received 8 June 2020; Received in revised form 15 July 2020; Accepted 22 July 2020
Available online 25 July 2020

Wang et al. [11–15] to try to simulate all these hysteresis phenomena. In the current paper, the dynamic phenomenological model proposed in [11–15] is employed to simulate the hysteretic dynamics of single-crystal structures, and lattice defects theory is introduced and incorporated into the model to capture the ferroelectric fatigue hysteretic dynamics. The paper is organized as follows. A brief introduction of Landau theory and mechanism of the current model are described in section 2. A description of macroscopic fatigue to be simulated by the current model is presented in section 3. In section 4, the hysteretic dynamics of ferroelectric fatigue are analyzed and simulated with the proposed model. Finally, in section 5, the simulation results of ferroelectric fatigue are compared with existing experimental results in both coupled and decoupled systems. Concluding remarks are presented in section 6.

2. Hysteretic model

In this study, Landau theory is employed to simulate the hysteresis loops of ferroelectric ceramics in the quasi-one-dimension, for the sake of simplicity. The hysteresis phenomena are regarded as the consequences of polarization orientation switching [15] as have been done in Ref. [12,13]. In a quasi-one-dimensional situation, there are three different polarization orientations (two 180° switching orientations and one Non 180° switching orientation), which are associated with the three local minima of the Landau free energy function, which is a non-convex function by Landau theory [11]. The Landau free energy function in the current paper is as follow:

$$F_L(P) = \frac{a_2}{2}P^2 + \frac{a_4}{4}P^4 + \frac{a_6}{6}P^6, \tag{1}$$

where P is the polarization of ferroelectrics; a_2, a_4 and a_6 are parameters that denote the Landau coefficients. Considering the electro-mechanical coupling effects and the damping effects during the switching processes, the energy function can be constructed as follow:

$$\Psi(P,\varepsilon) = \frac{a_2}{2}P^2 + \frac{a_4}{4}P^4 + \frac{a_6}{6}P^6 + \frac{k}{2}\varepsilon^2 + \frac{b}{2}\varepsilon P^2 - EP - \varepsilon\sigma, \tag{2}$$

where ε is the strain; b is the electromechanical coupling coefficient and k is linear elastic constant; τ_p and τ_ε are relaxation parameters related to the rate-dependence of the material. Based on the above energy function, the phenomenological model can be derived.

2.1. Single-crystal model

The model for the fatigue will be constructed by using the single crystal model. Therefore, Landau theory is employed to mimic the single-crystal polarization switching. Two time-dependent equations could be obtained to simulate the polarization orientation switching:

$$\frac{dP}{dt} = -\frac{1}{\tau_p}\frac{\partial\Psi}{\partial P}, \tag{3.a}$$

$$\frac{d\varepsilon}{dt} = -\frac{1}{\tau_\varepsilon}\frac{\partial\Psi}{\partial\varepsilon}. \tag{3.b}$$

The governing equation in this section can be obtained as follows [11–15]:

$$\tau_p\frac{dP}{dt} + a_2P + a_4P^3 + a_6P^5 + b\varepsilon P - E = 0, \tag{4.a}$$

$$\tau_\varepsilon\frac{d\varepsilon}{dt} + k\varepsilon + \frac{1}{2}bP^2 - \sigma = 0. \tag{4.b}$$

2.2. Polycrystalline model

The simulations for hysteresis loops in ceramic are far more complex than those of single-crystal ones. Ceramic can be regarded as a certain combination of various single-crystal domains, and the behaviors of the ceramic are assumed to be represented by a certain kind of combination of all these domains. It has been illustrated in Ref.14 that each grain in the ceramic could be characterized by an angle θ, which is the angle between the external field and its principal axis. As mentioned in [15], the governing equations of single grains are as follows:

$$\tau_p\frac{dP_\theta}{dt} + a_2P_\theta + a_4P_\theta^3 + a_6P_\theta^5 + b\varepsilon_\theta P_\theta - E\cos\theta = 0, \tag{5.a}$$

$$\tau_\varepsilon\frac{d\varepsilon_\theta}{dt} + k\varepsilon_\theta + \frac{1}{2}bP_\theta^2 - \sigma\cos\theta = 0, \tag{5.b}$$

where P_θ and ε_θ represent the local polarization and strain in the single grain respectively. For the sake of convenience in engineering applications, the polarization and strain can be approximated by using the Gaussian quadrature formulas as follows:

$$P = \int_\theta P_\theta w(\theta)\cos\theta\bullet d\theta = \int_\theta P_\theta\lambda(\theta)\bullet d\theta = \sum_{i=1}^{M} P_i\lambda(\theta_i)w_i = \sum_{i=1}^{M} P_iW_i, \tag{6.a}$$

$$\varepsilon = \int_\theta \varepsilon_\theta w(\theta)\cos\theta\bullet d\theta = \int_\theta \varepsilon_\theta\lambda(\theta)\bullet d\theta = \sum_{i=1}^{M} \varepsilon_i\lambda(\theta_i)w_i = \sum_{i=1}^{M} \varepsilon_iW_i, \tag{6.b}$$

where $w(\theta)$ is the volume percentage of the grain with angle θ; $\lambda(\theta)$ is the density function; w_i is the weight coefficient of i^{th} Gaussian quadrature term; W_i is the coefficient including both w_i and $\lambda(\theta_i)$.

The governing equations for the hysteretic dynamics of ceramics are formulated as follows:

$$\tau_p\frac{dP_i}{dt} + a_2P_i + a_4P_i^3 + a_6P_i^5 + b\varepsilon_iP_i - E\cos\theta_i = 0, \tag{7.a}$$

$$\tau_\varepsilon\frac{d\varepsilon_i}{dt} + k\varepsilon_i + \frac{1}{2}bP_i^2 - \sigma\cos\theta_i = 0, \tag{7.b}$$

$$P = \sum_{i=1}^{M} P_iW_i, \tag{7.c}$$

$$\varepsilon = \sum_{i=1}^{M} \varepsilon_iW_i. \tag{7.d}$$

More details about the model with figures can be referred to Ref. [11–15].

3. Hysteretic dynamics

It is not a trivial task to characterize the changes of hysteresis loops associated with the fatigue degradation phenomenon with a phenomenological model, since both the height and width of the fatigue hysteresis loops are changing during the process. The traditional phenomenological model such as the Preisach model can merely capture the hysteresis changes in height by controlling the value of density function. The hysteresis changes in width are still an unsolved problem. It will be shown here that this task could be fulfilled by using the proposed model.

According to the simulation of the time-dependent hysteretic loops as presented in previous publications [14,15], a fatter or thinner hysteresis loop can be obtained by the current model. Two simulations are performed to illustrate the capability of the model for varied hysteresis loops, and the results are presented in Fig. 2 and Table 1. In Fig. 2.a, it is shown that the width of the simulated hysteresis loops could be adjusted by tuning the value of the relaxation coefficient τ_p. Meanwhile, in Fig. 2.b, it is shown that the height of the simulated hysteresis loops can be adjusted by tuning Landau coefficients (a_2, a_4 and a_6). It is illustrated clearly from Fig. 2.b that those terms, such as $\tau_pc(t)^\alpha$, $a_2c(t)$, $a_4c(t)^3$ and $a_6c(t)^5$, make the equation very flexible to adjust the

Table 1
The model parameter values in Fig. 2.

Parameter	Value
τ_p	3.1773
a_2	0.012460
a_4	−0.040131
a_6	0.0052386

degradation of hysteresis loops in height, where $c(t)$ is the fatigue time-dependent function and $\propto$ needs to be estimated. The characteristics mentioned above will be applied as the strategies of parameter identification in section 5. The current model is unable to simulate changes in the size of three-dimensional crystal domains. For this reason, the current model has to use the change of the average polarization value of the crystal domain region in the original state to describe the physical spatial size change of the crystal domain in three dimensions. This process is the meaning of the fatigue time function proposed in the manuscript.

The defect density should have an influence on ferroelectrics' fatigue. It is unable to predict the influence of defect density on its fatigue directly for the current paper. However, according to the last paragraph, we can still get some hints to predict it. It is easily to think that the change of the average polarization value of the crystal domain region will be more drastically when the defect density becomes larger. Since the average polarization value represents the fatigue phenomenon in the current, the fatigue of ferroelectric is also influenced more seriously. And the changes of fatigue time function reflect the influence of defect density on its fatigue. However, due to the lack of experimental conditions, there is insufficient evidence to prove the above view. If possible, such remained question will be absolved in the following studies.

It should be noticed that due to changes in temperature and other conditions, the Landau potential of the ferroelectric will change. When the Landau potential changes, the identifications of Landau coefficients (a_2, a_4 and a_6) may change sometimes. The current model works in many situations. The abilities of the current model to simulate frequency-dependence [14,15] and stress-dependence [16,17] have been proved, so the identifications of Landau coefficients do not need to be changed due to the changes of the electrical or stress fields. However, the identifications have to be changed due to the changes in temperature, which means the current model only works in isothermal situation. And this flaw needs to be revised in subsequent studies.

4. Fatigue phenomenon and revised model

Ferroelectric fatigue is defined as the loss of switchable polarization with repeated polarization reversals [18]. The polarization and mechanical characteristics of ferroelectric ceramics are supposed to degrade during repeated electrical loading cycles, which means the hysteresis loops of the ceramics will become smaller with time. The microscopic mechanism responsible for this phenomenon is still not well established, but the macroscopic explanation is closely related to point defects [3]. Here, it is assumed that there are impurities exist in ferroelectric ceramics, which are attributed to the internal bias field in the domains under cyclically electrical loadings and gradually affect the dynamic behaviors of ceramics. As mentioned in section 2.2, the dynamic behaviors of ceramics are obtained by combining the behaviors of single-crystal domains with a certain weight which could be constructed as a density function.

Without losing the generality, it is assumed that only the dynamic behaviors of single-crystal domains will be changed during the fatigue

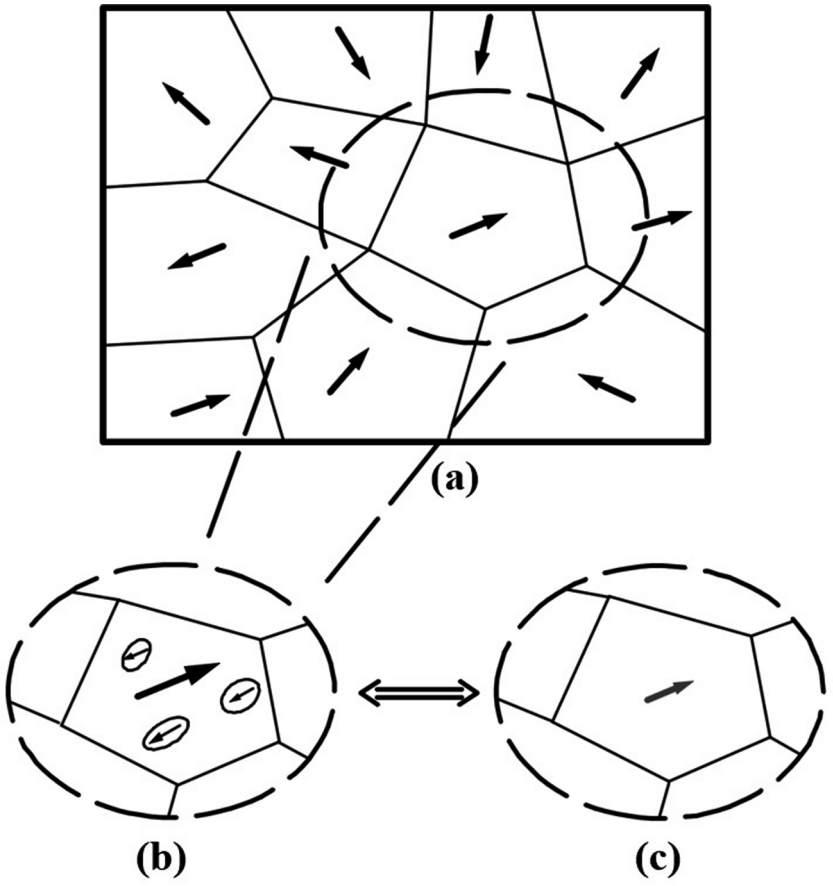

Fig. 1. (a) The distribution in a ferroelectric ceramic; (b) projection of the electric field in a grain with defects; (c) the equivalent electric field of this grain.

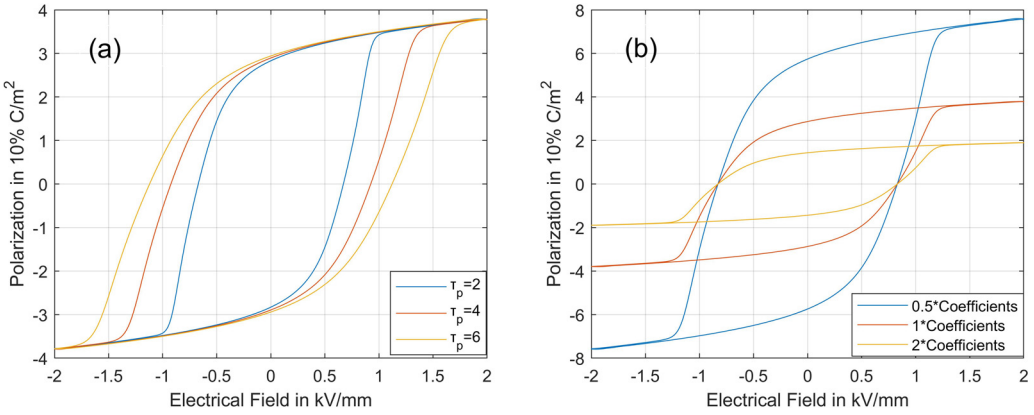

Fig. 2. Simulation hysteresis loops with (a) different polarization relaxation parameters τ_p; (b) different coefficients.

Table 2
Initial values and optimized values in the decoupled system.

Parameter	Initial Value	Optimized Value
τ_p	0.0012001	0.0014206
a_2	−0.00091784	−0.0012295
a_4	−0.000065491	−0.000044694
a_6	0.000000041243	0.000000033363
α	0.029646	0.025930
β	0.34283	0.40910
γ	0.91522	0.98896
mm	−2.0000	−1.9502
m_1	0.2500	0.24580
m_2	0.7500	0.75420
c	0.0010	0.00099923
d_1	10,000	9216.0
d_2	10,000	10,000

process because the effect of point defect will directly change the polarization switching itself. On the other side, the density function will be kept unchanged, since it represents the distribution of various grains with different principal axis, which certainly will not be changed by point defects. The detailed explanation of this assumption could be made easier by referring to Fig. 1. As shown in the figure, the ceramic impurities gradually appear inside some grains (which could be regarded as single crystal) when repeated polarization reversals are induced by repeated external loading cycles. Meanwhile, the un-switchable polarization value gradually accumulated and finally reaches saturation. This accumulation of un-switchable polarization therefore slowly decreases the switchable polarization to a limit value. When the accumulation of the un-switchable polarization is taken into account into the hysteretic dynamics, degradation will occur in the hysteresis loops, which is responsible for the fatigue phenomenon.

To model this phenomenon, each parameter should be adjusted in a

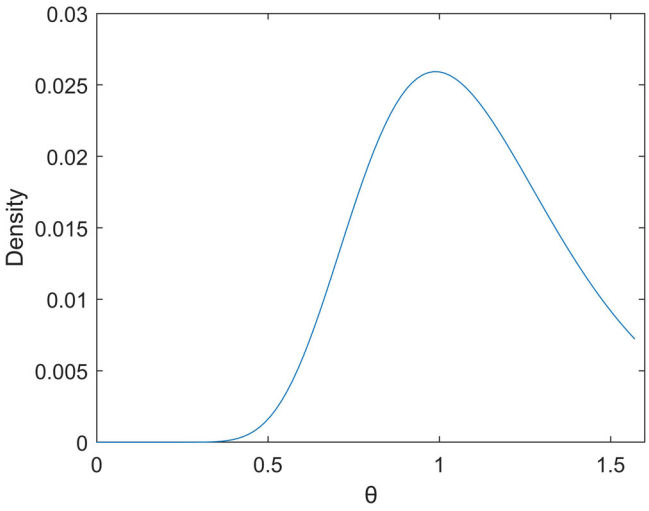

Fig. 4. Density function identified by using the experimental data.

specific way such that the number of repeating reversible polarization switching cycles should be taken into account. Here for the sake of convenience and simplicity, a time function is introduced to play the role of the discrete number of polarization switching cycles, which is a reasonable replacement since external loadings on the ferroelectric ceramics are mono-frequency ones. This parameter adjustment should be applied to the modeling of both the degradations of polarization and strain simultaneously. By looking at the experimental curves of fatigue phenomena, the hysteresis loops of polarization decline at the beginning, and are slowly stabilized when the loading time is long enough and will reach the saturation at the end. Thus, the time functions for parameter adjustment in the equation for polarization are chosen as

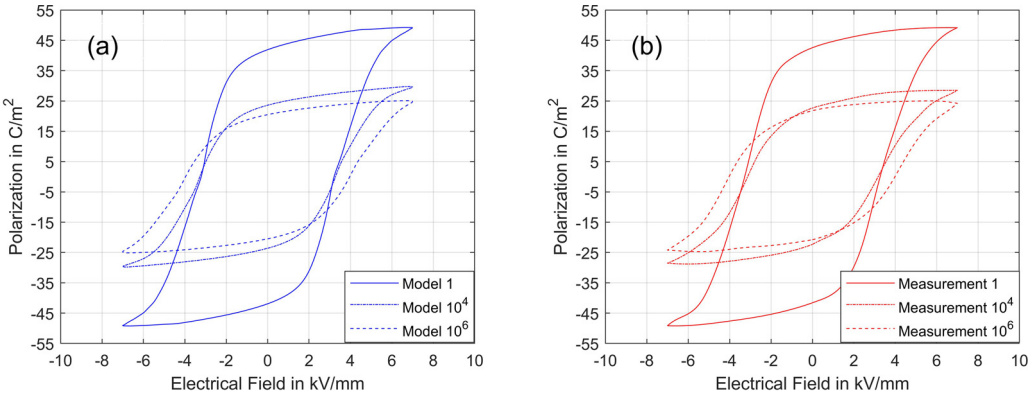

Fig. 3. Polarization hysteresis with fatigue. (a) Simulation results; (b) measurement results [18].

Table 3
Initial values and optimized values in the coupled system.

Parameter	Initial Value	Optimized Value
τ_p	2.7371	3.1773
a_2	0.013300	0.012460
a_4	−0.039700	−0.040131
a_6	0.0052000	0.0052386
τ_ε	0.062200	0.049327
b	−0.3521	−0.36507
k	6.2886	6.9030
α	0.010000	0.00991055
β	10,000,000	13,598,000
γ	4,000,000	4,944,100
mm	3.0000	3.0000
m_1	0.010000	608.91
m_2	0.30000	609.89
m_3	0.50000	628.67
m_4	0.90000	629.55
m_5	0.030000	0.022620
m_6	0.010000	0.010277
c_1	0.00080000	0.0014230
c_2	0. 0,060,000	0.0044263
c_3	0.0040000	0.0042625
d_1	−3000.0	−3698.8
d_2	−1000.0	−1051.1
d_3	30.000	36.295

$-\ m_1\tanh(c(t-d))+m_2$, which makes sure the switchable polarization value will converge to a certain value and the minor hysteresis loop can be obtained. To simplify the calculations, a modified hyperbolic tangent function is chosen here for the parameter adjustment, which is a pure empirical choice based on observation on the experimental data. The parameter adjustments for the equation of strain hysteresis are quite similar to the one for the equation of polarization, except for adjustment of the remnant strain, which is increasing while the other parameters are declining according to the data in Ref [21]. Therefore, the time function for the parameter adjustment for the equation of strain could be chosen as $-\ m_3\tanh(c_2(t-d_2))+m_4$, except the one for the remnant strain ε_{ri} which is chosen as $m_5\tanh(c_3(t-d_3))-m_6$. By introducing the above-mentioned parameter adjustment, the new governing equations are revised as follows:

$$\tau_p(t)\frac{dP_i}{dt}+a_2(t)P_i+a_4(t)P_i^3+a_6(t)P_i^5+2b(t)\varepsilon_iP_i-E\cos\theta_i=0, \tag{8.a}$$

$$\tau_\varepsilon(t)\frac{d\varepsilon_i}{dt}+k(t)\varepsilon_i+b(t)P_i^2-\sigma(t)\cos\theta_i=0, \tag{8.b}$$

$$P=\sum_{i=1}^{M}P_iW_i, \tag{8.c}$$

$$\varepsilon=\sum_{i=1}^{M}(\varepsilon_i+\varepsilon_{ri})W_i. \tag{8.d}$$

The time functions of Landau parameters are supposed to be identical in each to simplify the calculations. The values obtained by the original model in section.2 after one cycle hysteresis calculations are treated as initial values.

5. Numerical simulation and validation

Because the fatigue phenomena under prolonged loadings are very common in engineering applications, therefore numerical simulations are performed for those cases where the loadings are prolonged. Two numerical simulations of 94BNT-6BT ceramics [19] and PZT ceramics [21] are presented to illustrate the fatigue hysteresis. The simulated hysteresis loops with fatigue phenomena are compared with their experimental counterpart. Although the simulated material is three-

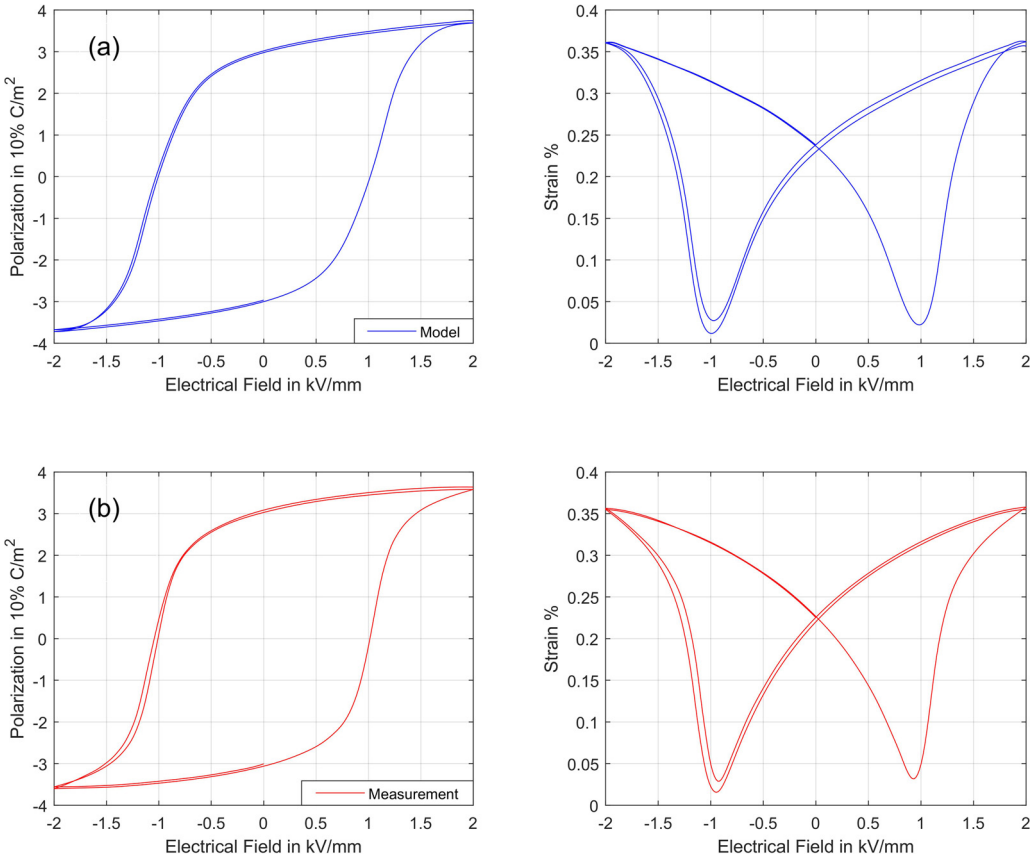

Fig. 5. Polarization and strain hysteresis loops with fatigue. (a) Simulation results; (b) measurement results [20].

dimensional, the measurement direction by researchers can be one-dimensional, and its projection in the measurement direction is still one-dimensional. That is to say, to a certain extent, the one-dimensional model can simulate three-dimensional materials, but the accuracy of the model will be slightly lacking. In fact, other influence of three-dimensional is all contribute to the 90°switching in the current paper. The fatigue time function in this paper is closely related to the influence of 90°switching in 3-D situation. In this section, the trapezoidal rule is used for solving the ordinary differential equations in Eq.8. For the simulations, the density function W_i is simplified to a log-normal density function in this section [15]:

$$W_i = \alpha e^{-[ln(\theta_i/\gamma)/\beta]^2}, \tag{9}$$

where α, β, and γ are the parameters need to be identified. To identify all the parameters, the following strategy is applied here:

$$\min_{\text{mod.para.}} G = \sum_{i=1}^{N} \left(\left(\frac{\widetilde{P}_i - P_i}{P_{magnitude}} \right)^2 + \left(\frac{\widetilde{\varepsilon}_i - \varepsilon_i}{\varepsilon_{magnitude}} \right)^2 \right), \tag{10}$$

where N is the number of data samples.

5.1. Decoupled polarization hysteresis with fatigue

Because, in many engineering applications, only the electric polarization response of the ferroelectric ceramics under the electrical field is of interest, therefore the model proposed in the above section could be simplified and the equation for the strain response could be ignored. In other words, it is meaningful to study the decoupled system with only polarization involved. By doing so, the simplified model could be recast into the following:

$$\tau_p(t)\frac{dP_\theta}{dt} + a_2(t)P_\theta + a_4(t)P_\theta{}^3 + a_6(t)P_\theta{}^5 - E\cos\theta = 0, \tag{11.a}$$

$$P = \sum_{i=1}^{M} P_i W_i, \tag{11.b}$$

$$\min_{\text{mod. para.}} G = \sum_{i=1}^{N} (\widetilde{P}_i - P_i)^2. \tag{12}$$

For comparison, the experimental results of 94BNT-6BT ceramics presented in Ref. [19] is chosen, and all the model parameters are estimated by using the presented experimental data. The angle θ is discretized by using 100 values in $[0,\ 0.5\pi]$. The parameter identification strategy is as follows:

1 The initial values of the fatigue time functions

$f(t) = -m_1\tanh(c(t-d_1)) + m_2,$

$\tau_p(t) = \tau_p{}^* f(t)^{'},$

$a_2(t) = a_2/f(t),$

$a_4(t) = a_4/f(t)^3,$

$a_6(t) = a_6/f(t)^5,$

are identified with the point values related to the max external loading of the hysteresis, where $f(t)^{'}$ is the function based on $f(t)$ and it will be identified in the following steps;

2 The initial values of single-crystal parameters τ_p, a_2, a_4 and a_6 are identified by using the experiment data;
3 The initial values of density function α, β and γ are identified by the polycrystalline model;
4 The full optimization problems in eq.10 with the initial values obtained in step 1,2,3 are carried out to get the final parameter values. And all the estimated values are listed in Table 2.

The simulation results are presented as hysteresis loops in Fig. 3 (a). In this case, the function $f(t)^{'}$ is defined as $(-m_1\tanh(c(t-d_2)) + m_2)^{mm}$, and the estimated density function is plotted in Fig. 4. For the comparison purpose, the experimental hysteresis loops with fatigue phenomena are also presented in Fig. 3 (b). By comparing the simulation and experimental hysteresis loops, which are plotted with different loading cycle numbers, it is illustrated very clearly that, when the number of loading cycles is increased, the simulated hysteresis loops become fatter and shorter than the one of the first cycle. The simulated hysteresis loops after 10,000 cycles agree very well with its experimental counterpart, so does that after 1,000,000 cycles. This observation indicates clearly that the hysteretic behavior with fatigue phenomenon due to prolonged loading is successfully captured by the proposed model. It is worth noting that the candidate density function for the simulation is not unique. A more deliberate choice of the density function will potentially produce a more accurate result [20], but with a cost of more demanding on the computational resource. The reason for choosing the current density function here is that it has only 3 parameters to be estimated and remarkably reduced the calculation time compared to a more deliberate density function.

5.2. Coupled polarization and strain hysteresis with fatigue

Since the aim of the current model is to simulate the change of the hysteretic loops associated with the fatigue phenomenon, the changing trend will play an important role in analyzing. The changing trend of hysteresis loops is particularly important for experimental investigation on fatigue since it is very demanding either in terms of time or other aspects when the loading cycle is very large. Therefore it will be meaningful to approximate the changing trend by using the hysteresis loops in the first few cycles. Here the first and second cycles of the hysteresis loops will be simulated and compared with their experimental counterparts. For the simulation, the fully coupled model given in Eq.(8) will be used, the numerical results will be compared with the experimental polarization and strain hysteresis loops for PZT ceramics, which is taken from Ref. [21]. For the simulation, the angle θ is discretized by using 100 values which are evenly distributed in $[0, 0.35\pi]$. The strategy for parameter identification in the coupled system is almost the same as the previous one, but the model parameters in the equation for the strain should be identified after the polarization ones. The total strain values will be separated into two parts: strain and remnant strain. The strain values will be decreased while the remnant strain will be increased. The fatigue time functions of these two parts are chosen as $-m_3\tanh(c_2(t-d_2)) + m_4$ and $m_5\tanh(c_3(t-d_3)) - m_6$. The fatigue time function of polarization is chosen to $-m_1\tanh(c_1(t-d_1)) + m_2$. The function $f(t)^{'}$ is chosen as $(-m_1\tanh(c_1(t-d_1)) + m_2)^{mm}$ in this section. Again, these choices are empirical. The algorithm for the estimation could be described as follows:

1 Repeat the steps 1–2 in section 5.1 to obtain the initial values of polarization hysteresis, such as mm, m_1, m_2, A, B, τ_p, a_2, a_4 and a_6;
2 The initial values of b and k are identified by the following reduced relation [14]: $\varepsilon = -\frac{b}{k}P^2 + \frac{\sigma}{k}$;
3 The initial values of fatigue time functions $-m_3\tanh(c_2(t-d_2)) + m_4$ and $m_5\tanh(c_3(t-d_3)) - m_6$ are identified with strain hysteresis;
4 The optimization problems of the coupled single-crystal model are carried out with initial values obtained by step 1–3;
5 The initial values of density function α, β, and γ are identified by the polycrystalline model;
6 All the parameter values are identified with the initial values obtained in steps 1−5. And all the values are listed in Table 3.

By using the estimated model parameters, the coupled polarization and strain hysteresis loops are simulated for the first and second loading

cycles. The simulated hysteresis loops are presented in Fig. 5. Again, for comparison purposes, the experimental polarization hysteresis curves and strain butterfly curves are also presented in the same figure, in different plots side by side with the simulated ones. It is verified by the simulation that, both the hysteresis loops and the butterfly loops at the second cycle become smaller than the loops at the first cycle, which means both polarization and strain are declining along with the electrical loading cycle. Meanwhile, the highest points of the butterfly loops keep almost stable, which indicates that the mechanical properties of materials are roughly unchanged. By comparing the simulated and experimental hysteresis loops and butterfly loops, it is clearly shown that the simulation result fits very well with the experimental curves. In both experimental and numerical loops, the fatigue phenomenon is identified by the decline of the hysteresis and butterfly loops.

By comparing the simulated hysteresis loops and butterfly loops with the experimental one, it is verified in both cases, a very large number of loading cycles and the first two cycles, the proposed model is capable of capturing the degradation of the loops caused by fatigue phenomenon.

6. Conclusion

In the current paper, a macroscopic phenomenological model has been proposed to characterize the fatigue hysteresis in ferroelectric ceramics. Time functions for model parameter adjustment have been introduced in the governing equation to account for the degradation of polarization and strain. Numerical simulations of hysteresis and butterfly loops with fatigue phenomena are presented. It has been illustrated by comparisons between the simulation results and their experimental counterparts are performed. The capability of the proposed model for characterizing the hysteretic dynamics with the fatigue phenomenon is verified.

Data availability

The raw data required to reproduce these findings cannot be shared at this time due to legal or ethical reasons. The processed data required to reproduce these findings are available to find in the current paper.

Declaration of Competing Interest

The authors declare that they have no known competing financial interests or personal relationships that could have appeared to influence the work reported in this paper.

Acknowledgments

This work has been supported by the National Natural Science Foundation of China (Grant No. 51575478 and Grant No. 61571007), the National Sciences and Engineering Research Council (NSERC) of Canada, and the Canada Research Chair Program. RM is also acknowledging support of the BERC2018-2021 program and Spanish Ministry of Science, Innovation, and Universities through the Agencia Estatal de Investigacion (AEI) BCAM Severo Ochoa excellence accreditation SEV-2017-0718.

References

[1] M. Kamlah, Ferroelectric and ferroelastic piezoceramics – modeling of electromechanical hysteresis phenomena, Contin. Mech. Thermodyn. 13 (2001) 219–268.
[2] D.A. Hall, Review Nonlinearity in piezoelectric ceramics, J. Mater. Sci. 36 (2001) 4575–4601.
[3] Y.A. Genenko, J. Glaum, M.J. Hoffmann, K. Albe, Mechanisms of aging and fatigue in ferroelectrics, Mater. Sci. Eng. B-Adv. 192 (2015) 52–82.
[4] T. Schenk, E. Yurchuk, S. Mueller, U. Schroeder, S. Starschich, U. Böttger, T. Mikolajick, About the deformation of ferroelectric hystereses, Appl. Phys. Rev. 1 (2014) 041103.
[5] E. Sapper, R. Dittmer, D. Damjanovic, E. Erdem, D.J. Keeble, W. Jo, T. Granzow, J. Rödel, Aging in the relaxor and ferroelectric state of Fe-doped (1-x)(Bi1/2Na1/2) TiO3-xBaTiO3 piezoelectric ceramics, J. Appl. Phys. 116 (104102) (2014).
[6] T. Zheng, H. Wu, Y. Yuan, X. Lv, Q. Li, T. Men, C. Zhao, D. Xiao, J. Wu, K. Wang, The structural origin of enhanced piezoelectric performance and stability in lead free ceramics, Energy Environ. Sci. 10 (2017) 528–537.
[7] J. Hao, W. Li, J. Zhai, H. Chen, Progress in high-strain perovskite piezoelectric ceramics, Mater. Sci. Eng. R Rep. 135 (2019) 1–57.
[8] X. Lou, Polarization fatigue in ferroelectric thin films and related materials, J. Appl. Phys. 105 (2009) 024101.
[9] D. Damjanovic, Ferroelectric, dielectric and piezoelectric properties of ferroelectric thin films and ceramics, Rep. Prog. Phys. 61 (1267) (1998).
[10] G. Sih, J. Zuo, Multiscale behavior of crack initiation and growth in piezoelectric ceramics, Theor. Appl. Fract. Mech. 34 (2000) 123–141.
[11] L. Wang, M. Willatzen, Nonlinear dynamical model for hysteresis based on non-convex potential energy, J. Eng. Mech. 133 (2007) 506–513.
[12] L. Wang, Hysteretic Dynamics Of Ferroelectric Materials Under Electro-Mechanical Loadings, American Society of Mechanical Engineers Digital Collection), 2008, pp. 189–195.
[13] L. Wang, R. Melnik, Control of coupled hysteretic dynamics of ferroelectric materials with a Landau-type differential model and feedback linearization, Smart Mater. Struct. 18 (2009) 074011.
[14] D. Wang, L. Wang, R. Melnik, A hysteresis model for ferroelectric ceramics with mechanism for minor loops, Phys. Lett. A 381 (2017) 344–350.
[15] X. He, D. Wang, L. Wang, R. Melnik, Modelling of creep hysteresis in ferroelectrics, Philos. Mag. 98 (2018) 1256–1271.
[16] L. Wang, R. Melnik, L. Fuzai, Stress induced polarization switching and coupled hysteretic dynamics in ferroelectric materials[J], Front. Mech. Eng. 6 (2011) 287–291.
[17] W.F. Chen, L.X. Wang, F.Z. Lv, Modeling of the stress-dependent hysteretic dynamics of ferroelectric materials[J], Adv. Mat. Res. 941-944 (2014) 606–609.
[18] A. Gruverman, O. Auciello, H. Tokumoto, Imaging and control of domain structures in ferroelectric thin films via scanning force microscopy, Annual review of materials science 28 (1998) 101–123.
[19] Z. Luo, J. Glaum, T. Granzow, W. Jo, R. Dittmer, M. Hoffman, J. Rödel, Bipolar and unipolar fatigue of ferroelectric BNT-based lead-free piezoceramics, J. Am. Ceram. Soc. 94 (2011) 529–535.
[20] D. Wang, L. Wang, R. Melnik, A differential algebraic approach for the modeling of polycrystalline ferromagnetic hysteresis with sub-loops and frequency dependence, J. Magnet. Magnet. Mater. S0304885316302281 410 (2016) 144–149.
[21] M.-A. Weber, M. Kamlah, D. Munz, Experimente zum Zeitverhalten von Piezokeramiken: FZKA-6465 and Institution, Institut für Materialfors hung (IMF), Karlsruhe, 2000.